Novel Fabrication of Engineered Nano-Selenium Incorporated Hydrogel for Potential Therapy and Care and of Acute Myocardial Infarction

Jianmei Li (jianmeili715@yahoo.com)
Huaihe Hospital of Henan University https://orcid.org/0000-0001-7813-3047
Pengfei Wang
The First People's Hospital of Zhengzhou

Research Article

Keywords: Myocardial infarction, Selenium, Hydrogel, Inflammatory factors, In vivo cardiac healing.

Posted Date: May 17th, 2021

DOI: https://doi.org/10.21203/rs.3.rs-508511/v1

Abstract

Recent years, the cardiac vascular disease has arisen owing to acute myocardial infarction (MI) and heart failures leads to death worldwide. Various treatments are available for MI in modern medicine such as implantation of devices, pharmaceutical therapy, and transplantation of organs, nonetheless it has many complications to find an organs donor, devices for stenosis, high intrusiveness and long-time hospitalization. To overcome these problems, we have designed and developed a novel hydrogel material with combination of Se NPs loaded poly(ethylene glycol)/tannic acid (PEG/TA) hydrogel for the treatment of acute MI repair. Herein, Se NPs was characterized by the effective analytical and spectroscopic techniques. *In vitro* cell compatibility and anti-oxidant analyses were examined on human cardiomyocytes in different concentrations of Se NPs and appropriate Se NPs loaded hydrogel samples to demonstrate its greater suitability into *in vivo* cardiac applications. *In vivo* investigations of MI mice models injected with Se hydrogels established that LV wall thickness was conserved significantly from the value of 235.6 μm to 390 μm. Addition that, the relative scar thickness (33.6 %) and infarct size (17.1 %) of the MI model was enormously reduced after injection of Se hydrogel when compared to the Se NPs and control (MI) sample, respectively, which confirmed that Se introduced hydrogel have greatly influenced on the restoration of infarcted heart. Based on the investigated results of the nanoformulated samples, it could be a promising material for future generations treatment of acute myocardial infarction and cardiac repair applications.

Research Highlights

Design of novel combination of Se NPs loaded poly(ethylene glycol)/tannic acid conductive hydrogel

The prepared material provides favourable cell compatibility and anti-oxidant abilities

Hydrogel samples significantly influenced on *In vitro* pro- and anti-inflammatory behaviours

It could be developed hydrogel promises of outstanding efficiency for the treatment of acute myocardial infarction

1 Introduction

Cardiovascular diseases are an important health problem and it’s a major cause of morbidity and mortality worldwide [1, 2]. Myocardial infarction (MI) is a most common cardiovascular disease, nearly 6.5 million individuals who are affected below 21 years by heart failure in U.S.A. MI was mainly caused by blocking of a coronary artery, which decreases the flow of blood to the parts of the heart leads to reduced oxygen supply to the heart muscle [3]. Although, development in the therapy of MI by medicine; bypass surgery and stent placement, the therapy of heart failure, which arises as an outcome of the loss of viable myocardial tissues and following tissue remodeling, is still a difficult problem[4]. Since, cardiomyocytes are mortally differentiated cells with the least rejuvenation ability; heart transplantation is presently the only preference treatment for the final stage heart diseases[5].

Novel treatments for MI are mandatory to convene this considerable clinical demand. Therefore, stem cell therapy[6][7] and cardiac tissue engineering for cardiovascular disease has in recent time increased broad attention[8]. The direct injection of stem cells leads to imperfect initial and continued stem cell engraftment at the preferred site due to outflow of the cells during inoculation and probably reduced cell viability due to cell injure acquired during the inoculation course, which can be accredited to the upset of transporting cells out of usual cell culture or to the harmful local microenvironment after inoculation. So, it's very important through the assist of proper biomolecules, cells, biomaterials and arrangement of these, cardiac tissue engineering plan to generate new functional cardiac tissue. Hydrogel based approach be capable of assist maintain stem cells following initial inoculation at the desired tissue place, as well as give guard to the inoculated cells and protect them from an instant attack, and thus recover their viability in the targeted tissue [9, 10].

Hydrogel work as a vehicle of stem cells and play smart due to simply invasive surgeries[11]. To facilitate intend the most favourable hydrogel, there are numerous considerations that necessitate to be measured counting the physical, material and biological properties[12]. The major thing that is necessary to deem in the construction of hydrogels in tissue engineering are the physical and material characteristics, mainly connected to hydrogel mechanics and the biological characteristics, concerned in cell adhesion, for the occasion. Preferably, the injectable hydrogels must be biocompatible and biodegradable to prevent triggering an immune response[13]. The engineered hydrogel, for cardiac inoculation should be dynamic, shrinkable and flexible with the ability to maintain periodic tightening and recreation. The hydrogel also is compromise well-vascularization so that the encapsulated cells in them obtain enough nutrients.

Electro active conductivity based materials were helpful for improving the communications among cardiomyocytes as well as enhancing the maturity of CMs and tissue rejuvenation[14]. Previously, remarkable studies have been made to construct conductive based biomaterials for treatment of MI that include electro active conductive materials such as carbon nanotubes, carbon quantum dots, grapheme, metal nano particles and conductive polymers blended into the selectable biomaterials, the conductivity will be enhanced [15]. Still, the Biosafety and metabolism of these electro active conductive particles are a huge anxiety after being inoculated into the myocardium. Selenium is a general traces element in the body and is essential to healthy nutrition, particularly in the formation of selenoproteins [16]. Deficiency of selenium has been associated with several diseases, including cardiovascular disease, keshan disease, etc. Selenium nanoparticles (Se NPs) were exhibited antioxidant activity and disease control properties and an immense deal of attention as a possible cardio protective agent[17]. Moreover, SeNPs revealed better scavenging effects of free radicals and protective effects against the oxidation of DNA with low toxicity and acceptable bioavailability[18]. Tetra aniline (TA), as an electroactive conductive material, acquires a well-defined arrangement, superior biocompatibility and admirable electroactivity close to that of polyaniline[19]. Moreover, TA is able to considerably decrease a few of the objectionable properties of the conducting polymers such as deprived solubility, reduced process ability and rough clearance[20, 21].In this study, an effort has been made to design an electroactive conductive injectable hydrogel with Se NPs on the delivery of cardiomyocytes for cardiac tissue engineering and nursing care application. We have effectively designed the PEG/TA injectable hydrogel with immensely dispersed and

spherical morphological exterior properties of Se NPs to examine the effect of Se NPs incorporated PEG/TA electroactive conductive injectable hydrogel on the cardiomyocytes.

2 Experimental Details

2.1 Ionic liquid mediated synthesis of Se NPs

Se NPs was prepared by ionic liquid mediated synthesis from precursor sodium selenite. For synthesis 15 mg of Na_2SeO_3 powder was dissolved in 50 mL of deionised water and stirred at room temperature for 15 minutes. Thereafter, 1 mL of ionic liquid [BMIM] BF_4 was added and continuously stirred for 1 hour to get homogenous solution. Then, 0.5 M of freshly prepared aqueous solution of $NaBH_4$ was added to an above solution in drop wise manner. After the addition, the colour of the solution was changed into orange and allowed to stir for 2 hours. The resulting solution was centrifuged at 12000 rpm for 10 minutes. The reddish orange precipitate was settled and washed once with ethanol, and dried for further analysis.

2.2 Synthesis of PEG/TA –Se NPs composite hydrogel

For synthesis, 30% wt of PEGDA was dissolved in DMSO and 2 wt % of TA in DMSO was mixed in the presence of triethylamine (TEA) with continuous stirring. TEA can act as a deacid reagent to improve the rate of reaction. The pH of the reaction mixture was maintained pH = 9 by the addition of (TEA) and then the mixture was heated at 100°C for 12 hours. After the completion of the reaction, the reaction mixture was extracted with ice cold diethyl ether in order to remove an unreacted monomer. After PEG was blended with TA, Se NPs was doped with PEG/TA composite, the schematic representation of synthetic procedure was depicted in Scheme 1.

2.3 Characterization techniques

Se NPs formation was confirmed by UV-Visible spectroscopy-Perkin Elmer LAMBDA 950 UV-VIS-NIR Spectrophotometer. Size and morphology of NPs was revealed using HRTEM: Jeol/JEM 2100. Functional group present in hydrogel composite was confirmed by MODEL Bruker TENSOR-27. Crystalline nature of NPs was examined using X-ray analysis technique-D8 Advance Bruker.

2.4 *In vitro* cytocompatibility

The cell survival of the cardiomyocytes treated with prepared nanoparticles and hydrogel was investigated by using cell proliferation (MTT) assay kit (Cell titer, Promega, USA) as followed by manufacture's protocol. In brief, cardiomyocytes (1×10^4) were cultured into 96-well plates and treated with different dose-related concentrations of prepared NPs and hydrogel samples for 24 h. After that, freshly prepared MTT assay (5 mg/mL) solution was added to individually treated cell culture plates. The MTT assay treated medium was separated and then DMSO was furtherly added after 4 h. Lastly, the absorbance of the MTT treated well was measured at 490 nm and cell survival percentage was quantitatively calculated and presented.

2.5 *In vitro* anti-oxidant activity

For quantitative measurement of ROS accumulation, the cardiomyocytes were cultured in well plates and incubated with freshly prepared DCFH-DA (10 mM) for 30 minutes at biological atmospheric condition (37°C) in the dark condition room. Then, cells were washed with PBS and treated with prepared nano formulated samples for 4 h. Treated cells were collected by centrifugation (9000 rpm) for 5 min and supernatant samples were observed and recorded under fluorescence spectroscopic technique at 530 nm.

2.6 *In vivo* myocardial infarction model

2.6.1. Animals

The male mice (9-week-old) were used to observe the MI induced inflammatory analysis and then those were divided into 4 groups; (i) sham group (control), (ii) MI (control), (iii) Se NPs and (iv) Se hydrogel treated groups. To induce MI of the *in vivo* models, the selected animal groups were anaesthetized by using chloral hydrate (4 %; 0.01 mL/g) under rodent ventilator as approved protocol of Animal care and International guidelines of animal procedures and ethical committee of Henan University, PR China. After that, the animal heart was exposed through the thoracotomy surgery procedure and myocardial infarction was induced artificially by the surgical obstruction of the LAD with sutures. To the treatment of prepared biomaterials, Se NPs and Se hydrogel were successfully injected at center of the infarction site by using surgical gauge needle. After injected treatments of hydrogels, the animal's surgery site was closed and were observed at suitable incubated environment. Then, animals with actions of severe LAD ligation and ineffective LAD ligations were excepted for next step of the *in vivo* observations.

2.6.2 Histological observations

The treated MI induced animals were sacrificed after 6 weeks and heart samples were separated and then buffered formalin was fixed before histopathology staining process. After that, Hematoxylin & Eosin (H&E) and Masson's trichrome (MTS) staining's were applied on squeeze of paraffin (5 μm) sections. Then, the degree of fibrosis and scar thickness & infarct size were quantitatively observed by left ventricular (LV) wall thickness using well-known method of Image-Pro Plus software. In brief, epithelial circumference of the LV wall and mean thickness of the fibrotic region were divided into 6 segments to estimate LV wall thickness and scar thickness, respectively as shown in H&E and MTS staining.

2.6.3 Measurements of mRNA expressions and cytokine productions

The mRNA expressions were quantitatively estimated by using total RNA molecules extracted from treated animal heart sample through TRIzol reagent method. The concentrations of RNA was observed and measured using spectrophotometer (Nanodrop 2000) and mined total RNA from each groups were transliterated reversely under RevertAid Transcriptase to synthesis cDNA. All the experimental observations were repeated in three times and recorded for the accurate values. The gene expressions levels were signified as following equation ($\Delta Ct = Ct^{gene} - Ct^{ref}$). The pro-inflammatory cytokines (TNF-α,

IL-18 and CCL2) of cultured cells (NIH3T3, iPSC-CMs (cardiomyocytes) and Raw 264.7) were observed in the presence and absence of LPS (1µg/mL) for 6 h after treated with prepared NPs and hydrogel in serum-free conditions. After treatment of LPS, the extracted supernatant from cell culture were collected and presentations of cytokines were estimated by using purchased pro-inflammatory cytokine ELISA Kit (NeoBioscince, PR China) as following exactly manufactures protocol.

2.7. Statistical analysis

Statistical value of the all-biological data was observed and calculated using the method of one-way ANOVA with assistance of SPSS software in belongings of all treated and untreated groups. The obtained value of $p < 0.05$ was considered to be statistically significant.

3 Results And Discussion

In this current work, we describe an effective approach for synthesis of PEG/TA-Se NPs hydrogel for cardiac tissue engineering application. Se NPs was prepared by ionic liquid mediated synthesis, then the particle formation was confirmed by UV-Visible spectroscopy. An absorption spectrum of sodium Selenite and Se NPs (after the reduction) was provided in Fig. 1

An overlapped spectrum displayed a peak at around 200 nm for precursor and a peak present at 265 nm which is due to formation of Se NPs using reducing agent $NaBH_4$. Comparing the spectrum for Na_2SeO_3 and absorption spectrum obtained for Se NPs in Fig. 1, the peak was shifted into 265 (red shift) which indicating the formation of nano selenium. Structural morphology of as prepared Se NPs was characterised by TEM studies. A small portion of colloidal solution of nano selenium was centrifuged at 12000 rpm, washed with ethanol in order to remove excess the ILs present in the solution. The reddish orange precipitate was settled and dispersed in ethanol for TEM analysis. Figure 1b showed a TEM image of Se NPs, the particles are almost spherical shape ~ 10 to15 nm respectively. Further, the crystalline nature of as prepared Se NPs was confirmed X-ray studies. The particles showed the peaks at 2 (value 23.3°, 28.5°, 41.2°, 43.5°and 44.4° which is corresponds to a plane lattice (100), (101), (110), (102) and (111) was a good match to the literature as shown in Fig. 1d respectively. In addition to that, SAED pattern of Se NPs depicted in Fig. 1c revealed the crystalline nature of NPs.

Besides, the FTIR spectra of tetra aniline (TA), PEG, PEG-Se NPs and PEG/TA-Se NPs was depicted in Fig. 2. Spectrum 2a showed a sharp peak at around 3500 cm^{-1} due to presence N-H stretching for the amine group in TA. The characteristic peak at 1568 cm^{-1} due to C = C stretching vibration of benzeniod structure. Moreover, the sharp observed at 1128 cm^{-1} was attributed to C-N bending vibration. Figure 2b displayed FT-IR spectrum for PEG, it showed a broad band at around 3500 cm^{-1} was predicted as OH stretching of the hydroxyl group. The peak present at wavenumber 1450 cm^{-1} to 1292 $cm^{-1}$is owing to scissor and bending vibration. Further the peak at 1256 cm^{-1} was attributed to C-O stretching from Alcohol present in PEG. The peak observed at 1180 cm^{-1} is C-O-C stretching, vibration which confirmed the presence of the ether linkage.

The FT-IR spectrum of PEG/TA-Se NPs hydrogel composite is closely resembled to a spectrum of PEG and TA is given in Fig. 2D, the main characteristic peaks for OH, C-O is stretching for Alcohol, ether was obtained in the spectrum D, Also a small sharp peak 1158 cm^{-1} for C-N bending vibration which revealed the existence of TA in ternary hydrogel composite. Based on theses FTIR results, we conclude the conjugation of PEG/TA in Se NPs vividly supported that PEG forms the ternary composite hydrogel. In addition to chemical characterisation, hydrogel composite formation was further confirmed by UV-Visible spectroscopy. Figure 2b exhibited an overlapped UV-visible spectrum of Se NPs, PEG/TA, and PEG/TA-Se NPs. We observe a peak at 265 nm for Se NPs and according to previous reports, an absorption band at around 300 nm in spectrum b for PEG-TA respectively. On the other hand, the spectrum c displayed an intense peak at 265 nm and a shoulder peak at 320 nm revealed grafting of Se NPs in PEG/TA hydrogel network.

Surface morphology of PEG hydrogel was examined in SEM analysis. Figure 3A showed the hydrogel surface was highly porous and fibrous in texture. However, this porosity will enhance the swelling behaviour of hydrogel. As seen in figure, shape of pores is spherical and ellipsoid with different diameter, it has a tendency to absorb high permeability for nutrients, oxygen and water soluble metabolites. After the incorporation of SeNPs in to hydrogel, the particles are embedded in the pores of hydrogel network considerably it will improve the mechanical properties. In addition to SEM studies, Se NPs doping was further confirmed through TEM analysis. Spherical shaped Se NPs were embedded on the surface of PEG/TA hydrogel composite is displayed in Fig. 4A and B showed the existence of NPs in hydrogel in another portion of grid.

Toxicity analysis of prepared hydrogel samples on cardiomyocytes

The cytocompatibility of the prepared nanoformulated hydrogel samples was primarily analysed by the treatment of dose-depended manner treatment of SeNPs (6.25, 12.5, 25 and 50 µg/mL) on the human cardiomyocytes (AC16). The cell viability results on dose-depended manner treatment of prepared nanoformulated samples are displayed in Fig. 5. The presented results of cell survival exhibited that Se NPs in lower concentrations and control samples was not significantly affected the cell viability ratio.

The cell survival experimental results were greatly used to measure the dose-depended influencing factors and favourable interactions between the prepared samples and treated cells (Fig. 5a and 5b). In addition, we have examined the damage of cardiomyocytes cell membranes through measurement of LDH level after treatment of prepared samples as exhibited in Fig. 5e. The observed data have been exhibited that significant increasing LDH level at higher concentrations when compared to lower concentration and control, which demonstrates appropriate concentration of Se nanoparticles could be highly suitable with cardiomyocytes cell survival. Importantly, the examination of ROS generation and oxidative stress efficiency is highly needful for the cardiac regeneration applications. As showed in Fig. 5c, the results from flow cytometry analysis of intracellular ROS generations exhibited that composited group of PEG-TA/Se was suggestively greater that bare group of Se NPs and control group. These investigations demonstrated that enhanced ROS generations was persuaded by interactions

between Se NPs and TA/PEG macromolecular structure. The anti-oxidant activity of the prepared samples on the AC16 was investigated by the SOD as shown in Fig. 5d. The analysis results demonstrated that intracellular SOD and GSH-Px level was decreased by inducing interactions between the Se NPs and TA-PEG.

In vivo examinations of MI-induced inflammatory responses after treatment of prepared hydrogel

To investigate therapeutic potential of the prepared hydrogel materials after MI, we examined an animal MI model with presence of permanent occlusion of coronary artery (LAD). The prepared Se NPs and Se hydrogel samples were individually injected on the myocardial infarction site after MI occlusion to observed therapeutic potential and regeneration ability. The microscopic observation of large occupation of collagen zone on the LV wall and infarct site as shown in Fig. 7 at control (PBS), which signifying the existence of extensively spread scar tissue. On the other hand, the MI models injected with Se hydrogel samples have exhibited that large myocardial tissue at MI site as displayed in Fig. 7 (A). Meanwhile these observations are strongly consistent with the results of LV wall thickness and relative scar thickness. The quantitative data showed LV wall thickness was conserved significantly from the value of 235.6 μm to 390 μm (Fig. 7B). Meanwhile, the relative scar thickness (33.6 %) and infarct size (17.1 %) of the MI model was enormously reduced after injection of Se hydrogel when compared to the Se NPs and control (MI) sample, respectively, as displayed in Figure (7C & 7D), which confirmed that Se introduced hydrogel have greatly influenced on the restoration of infarcted heart.

Though post-infarction inflammatory processes are played essentially in the heart healing mechanism, which mainly demonstrates excessive and upregulated inflammation provides negative effects and causes adversative pathological remodelling. During inflammation period (at beginning of 1–48 h after MI), the pro-inflammatory cytokines (TNF-α and IL-18) level have been significantly increasing and subsequently the levels of anti-inflammatory cytokines (IL-10 and TGF-b) also enthused to suppress over-expressions of inflammatory expressions. In the present study, we have examined those inflammatory cytokines that are possibly related to macrophage recruitment at infarcted regions to establish the activations of macrophages and functional heart regeneration as showed in Fig. 6. Primarily, we have analysed the chemokine and cytokines at infarcted heart regions, which are capable of engaging macrophages. On day 3, the pro-inflammatory factors and anti-inflammatory factors were upregulated in control samples (MI heart). Nevertheless, the hydrogel treated samples exhibited to specifically downregulated levels of mRNA level (Fig. 6a) and protein expressions (Fig. 6b) of pro-inflammatory factors (TNF-α and IL-18) and chemokines (CCL2) without influencing the anti-inflammatory factors, demonstrating that prepared hydrogel samples have probable anti-inflammatory efficiency and favourable pro-inflammatory effect on *in vivo* MI treatment. And we further examined the infiltration of macrophages in the infarcted hearts after macrophages recruitments and activation of CCL2 as exhibited in Fig. 6d and 6d1. The present investigation established that number of macrophages was significantly decreased after treatment of prepared hydrogel when compared to the control sample, which displays clear evidence of hydrogel has been prevents macrophages activations, which is possibly under downregulating CCL2.

In vivo analysis of pro-inflammatory cytokines (TNF-α, IL-18 and CCL2) expressions with treatment of hydrogels

The *in vivo* observations of inflammatory cytokines determined that prepared hydrogel samples greatly influenced for anti-inflammatory effects as exhibited in Fig. 8. In addition, we have examined the inflammatory cytokines responses on the cell types including NIH3T3 (Fig. 8a) and iPSC-CMs (Fig. 8b), which are involved in the MI-based healing process. The present investigation exhibited that hydrogel treatment on cell types have been significantly suppressed the mRNA and protein expressions of pro-inflammatory factors (TNF-α, IL-18 and CCL2) as showed in Fig. 8 (a). These *in vitro* analysis results provided additional support that role of inflammatory production of cytokines by *in vivo* treatment. To examination the hydrogel role in the inflammation-endorsed production of cytokines, we have observed *in vitro* inflammation analysis under LPS-induced inflammatory process. In this study, mouse macrophages (RAW 264.7) (Fig. 8c1-c3) were selected for inflammation examination because these similar types of cell type are involved in the myocardial healing process and also momentously responded LPS-based inflammatory investigations. The treatment of LPS onto the RAW 264.7 macrophages cells promisingly producing inflammatory cytokines (TNF-α, IL-18 and CCL2), which also established that production and upregulation of inflammatory cytokines levels on RAW 264.7 have been reduced after treatment of prepared hydrogel. The microscopic visualization of Raw 264.7 macrophages was presented in Fig. 8 (d) to establish regeneration ability of the prepared hydrogels. The observed results demonstrated that the treatment of hydrogel samples onto the LPS-induced macrophages cells have blocked the further accessibility of LPS with the cells. The presented results indicated that presented selenium nanoformulations into the hydrogel greatly influenced into the LPS-induced inflammatory response and provided strong anti-inflammation role.

4 Conclusion

In this present investigation, we have developed the TA/PEG hydrogel materials with assistance of Se Nanoparticles to improve cardiac regeneration efficiency after acute myocardial infarction. Modification PEG hydrogel matrix with TA and Se nanoparticles have been provided the effective porous morphology behaviours, which was confirmed by the SEM and TEM microscopic analyses. In vitro analyses were demonstrated that prepared hydrogel samples greatly influenced for anti-oxidant activity, suppressing pro-inflammatory factors and induced anti-inflammatory activity on the cardiomyocyte's cells, fibroblast cells and RAW 264.7 macrophages cells. *In vivo* MI models demonstrated that LV wall thickness was significantly preserved and the relative scar thickness and infarct size of the MI model was enormously reduced after injection of Se hydrogel when compared to the Se NPs and control (MI) sample, respectively, which confirmed that Se introduced hydrogel have greatly influenced on the restoration of infarcted heart. We assured that hydrogel designed with Se nano-topography could be effective tool for the future cell delivery vesicles and myocardial infarction treatment.

References

1. Cardiovascular disease review series (2011) 2011. doi:10.1002/emmm.201100182
2. Stewart J, Manmathan G, Wilkinson P, Primary prevention of cardiovascular disease: A review of contemporary guidance and literature, (2017) 1–9. doi:10.1177/2048004016687211
3. Lackland D, Heart Disease and Stroke Statistics — 2017 Update A Report From the American Heart Association (2017) doi:10.1161/CIR.0000000000000485
4. Venugopal JR, Prabhakaran MP, Mukherjee S, Dan K, Ramakrishna S, Venugopal JR, Prabhakaran MP, Biomaterial strategies for alleviation of myocardial infarction Biomaterial strategies for alleviation of myocardial infarction, (2012). doi:10.1098/rsif.2011.0301
5. Hajjar RJ, Hajjar RJ, Potential of gene therapy as a treatment for heart failure Find the latest version: Review series Potential of gene therapy as a treatment for heart failure, 123 (2013) 53–61. doi:10.1172/JCI62837.critically
6. Perin EC, López J, Methods of stem cell delivery in cardiac diseases, 3 (2006) 110–113. doi:10.1038/ncpcardio0447
7. Segers VFM, Lee RT, Stem-cell therapy for cardiac disease, 451 (2008) 937–942. doi:10.1038/nature06800
8. Zimmermann W, Melnychenko I, Eschenhagen T, Engineered heart tissue for regeneration of diseased hearts $, 25 (2004) 1639–1647. doi: 10.1016/S0142-9612(03)00521-0
9. Peña B, Laughter M, Jett S, Rowland TJ, Taylor MRG, Mestroni L, Park D (2018) Injectable Hydrogels for Cardiac Tissue Engineering 1800079:1–22. doi:10.1002/mabi.201800079
10. Hasan A, Khattab A, Islam MA, Hweij KA, Zeitouny J, Waters R, Sayegh M, Hossain M, Paul A, Injectable Hydrogels for Cardiac Tissue Repair after Myocardial Infarction, (2015) 1–18. doi:10.1002/advs.201500122
11. Li J, Mooney DJ (2016) Designing hydrogels for controlled drug delivery. Nat Publ Gr 1:1–18. doi:10.1038/natrevmats.2016.71
12. Pertici V, Pin-barre C, Rivera C, Laurin J, Gigmes D, Trimaille T, Degradable and injectable hydrogel for drug delivery in soft tissues, (2018). doi:10.1021/acs.biomac.8b01242
13. Nawaz S, Khan S, Farooq U, Haider MS, Ranjha M, Rasul A, Nawaz A, Arshad N (2018) Biocompatible hydrogels for the controlled delivery of anti-hypertensive agent: development, characterization and in vitro evaluation. Des Monomers Polym 5551:18–32. doi:10.1080/15685551.2018.1445416
14. Ashtari K, Nazari H, Ko H, Tebon P, Akhshik M (2019) Electrically conductive nanomaterials for cardiac tissue engineering. Adv Drug Deliv Rev 144:162–179. doi:10.1016/j.addr.2019.06.001
15. Lu H, Zhang N, Ma M, Electroconductive hydrogels for biomedical applications, (2019) 1–15. doi:10.1002/wnan.1568
16. Skalickova S, Sc M, Milosavljevic V, Sc M, Cihalova K, Sc M, Horky P, Ph D, Richtera L, Ph D, Adam V, Ph D (2020) Selenium nanoparticles as a nutritional supplement. Nutrition 33:83–90. doi:10.1016/j.nut.2016.05.001

17. Kong H, Yang J, Zhang Y, Fang Y (2014) International Journal of Biological Macromolecules Synthesis and antioxidant properties of gum arabic-stabilized selenium nanoparticles. Int J Biol Macromol 65:155–162. doi:10.1016/j.ijbiomac.2014.01.011
18. Uang BOH, Hang JIZ, Ou JIH, FREE RADICAL SCAVENGING EFFICIENCY OF NANO-SE IN VITRO, 35 (2003) 805–813. doi:10.1016/S0891-5849(03)00428-3
19. Cui H, Liu Y, Deng M, Pang X, Zhang P, Wang X, Chen X, Wei Y, Synthesis of Biodegradable and Electroactive Tetraaniline Grafted Poly(ester amide) Copolymers for Bone Tissue Engineering, (2012)
20. Atoufı Z, Zarrintaj P, Motlagh GH (2017) A Novel Bio Electro Active Alginate-Aniline Tetramer / Agarose Scaffold for Tissue Engineering: Synthesis, Characterization, Drug Release and Cell Culture Study. J Biomater Sci Polym Ed 5063:0–1. doi:10.1080/09205063.2017.1340044
21. Arioz I, Erol O, Bakan G, Dikecoglu FB, Topal AE, Urel M, Biocompatible Electroactive Tetra(aniline)-Conjugated Peptide Nano fı bers for Neural Di ff erentiation, (2018). doi:10.1021/acsami.7b16509

Figures

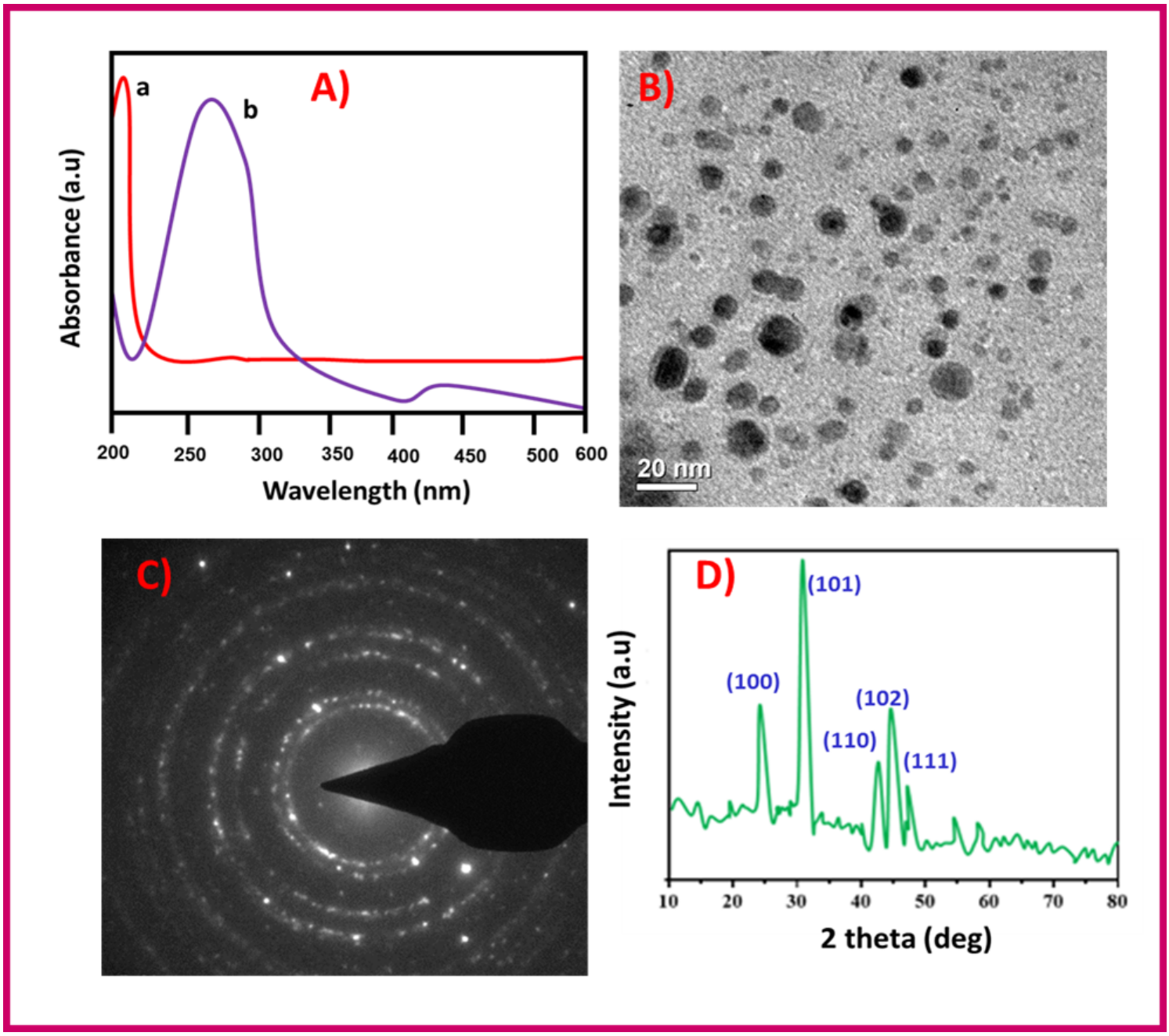

Figure 1

A. Absorption spectra of a) precursor sodium selenite b) Se NPs B) TEM image of Se NPs C) SAED pattern for Se NPs showed crystalline nature D) XRD pattern for Se NPs

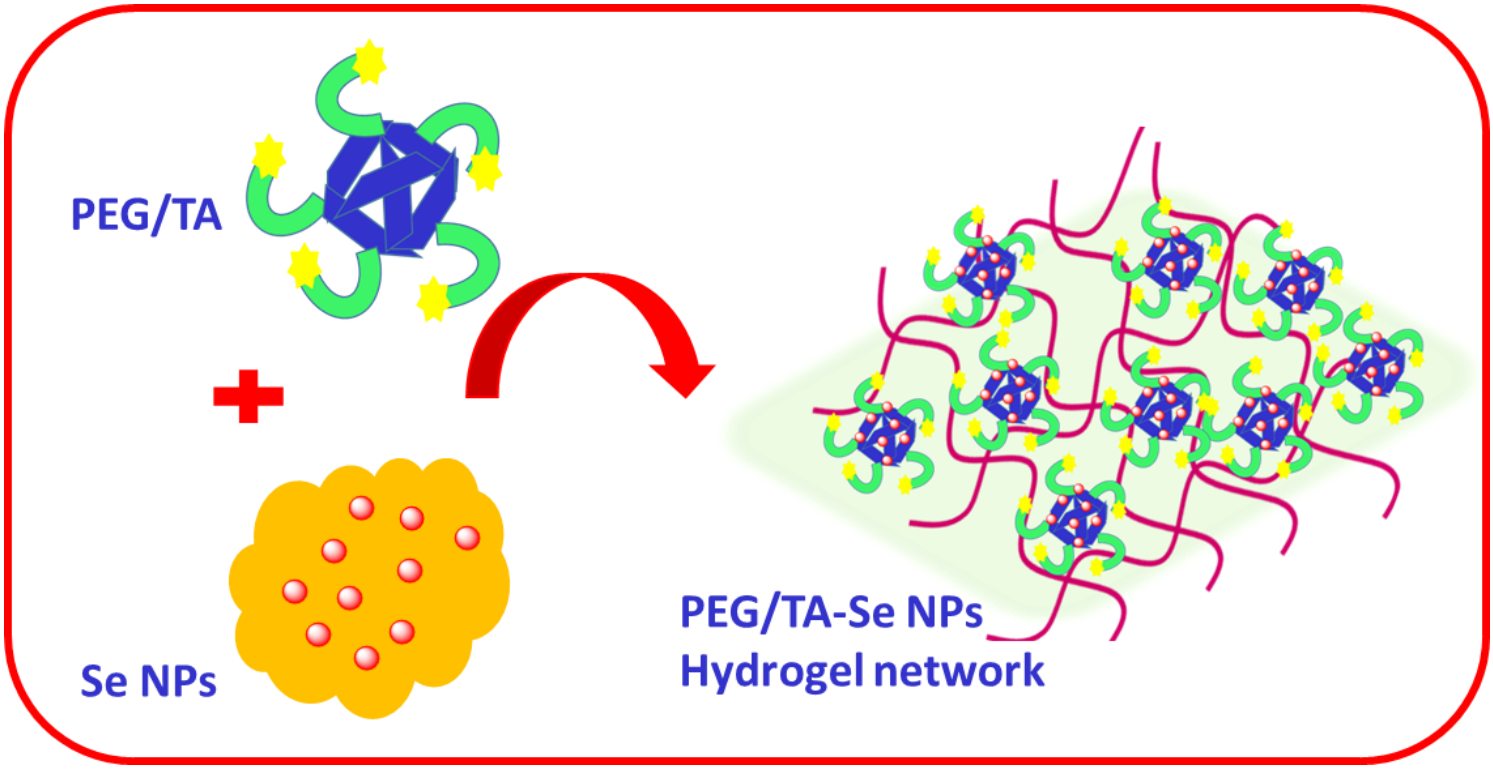

Figure 2

Schematic representation of synthesis of PEG/TA-Se NPs hydrogel

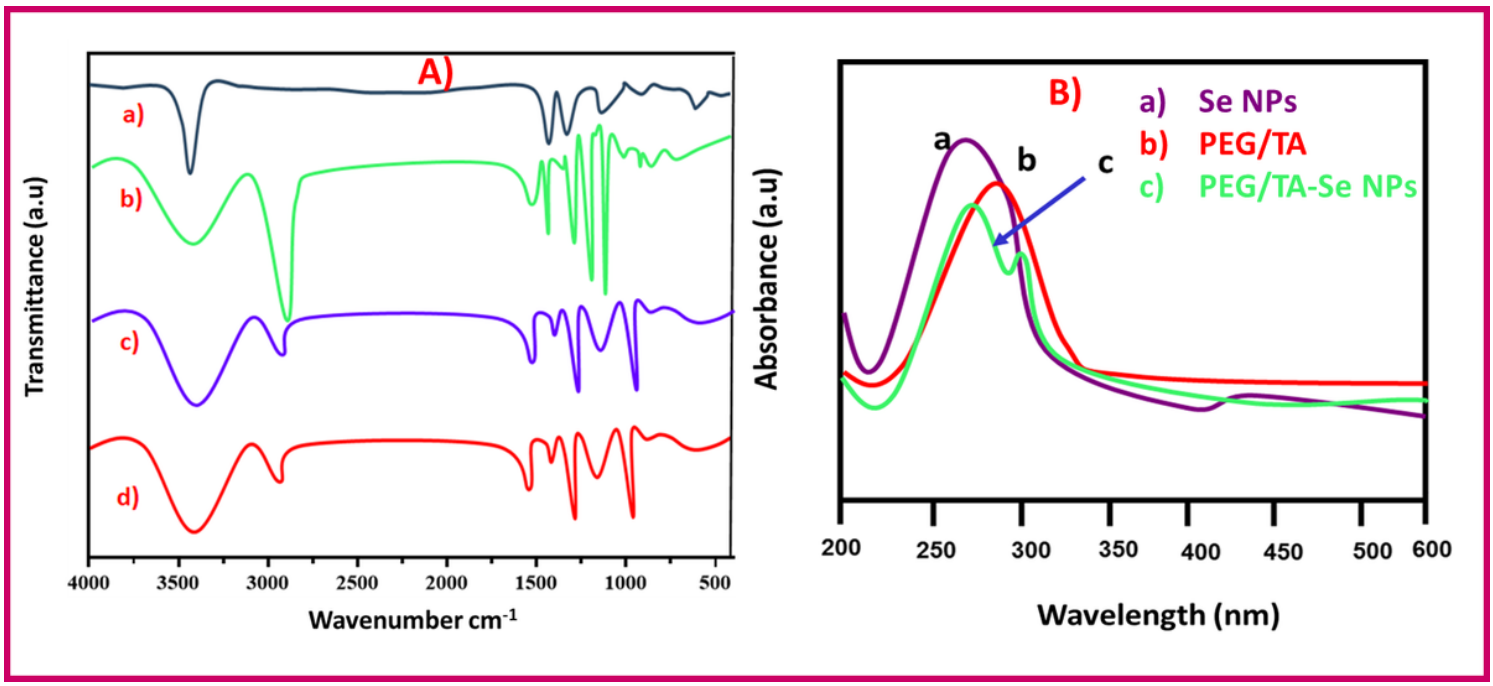

Figure 3

A) An overlapped FTIR spectrum for a) TA b) PEG C) PEG-Se NPs and D) PEG/TA-Se NPs 2B) UV-Visible spectrum for Se NPs, PEG-TA and PEG/TA-Se NPs.

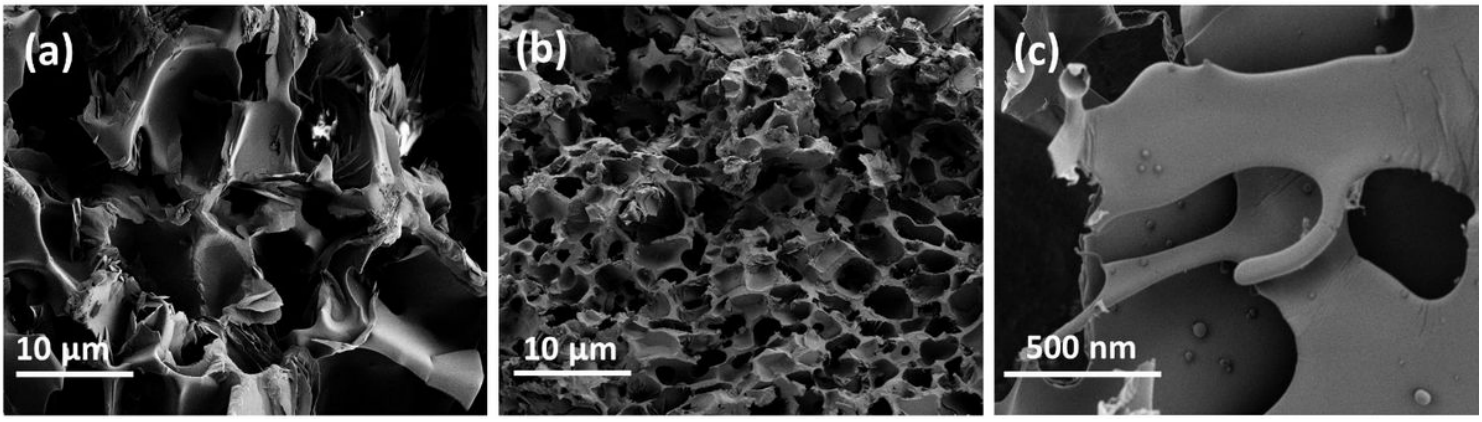

Figure 4

A) SEM image of PEG B) PEG/TA-Se NPs C) Expanded image of B.

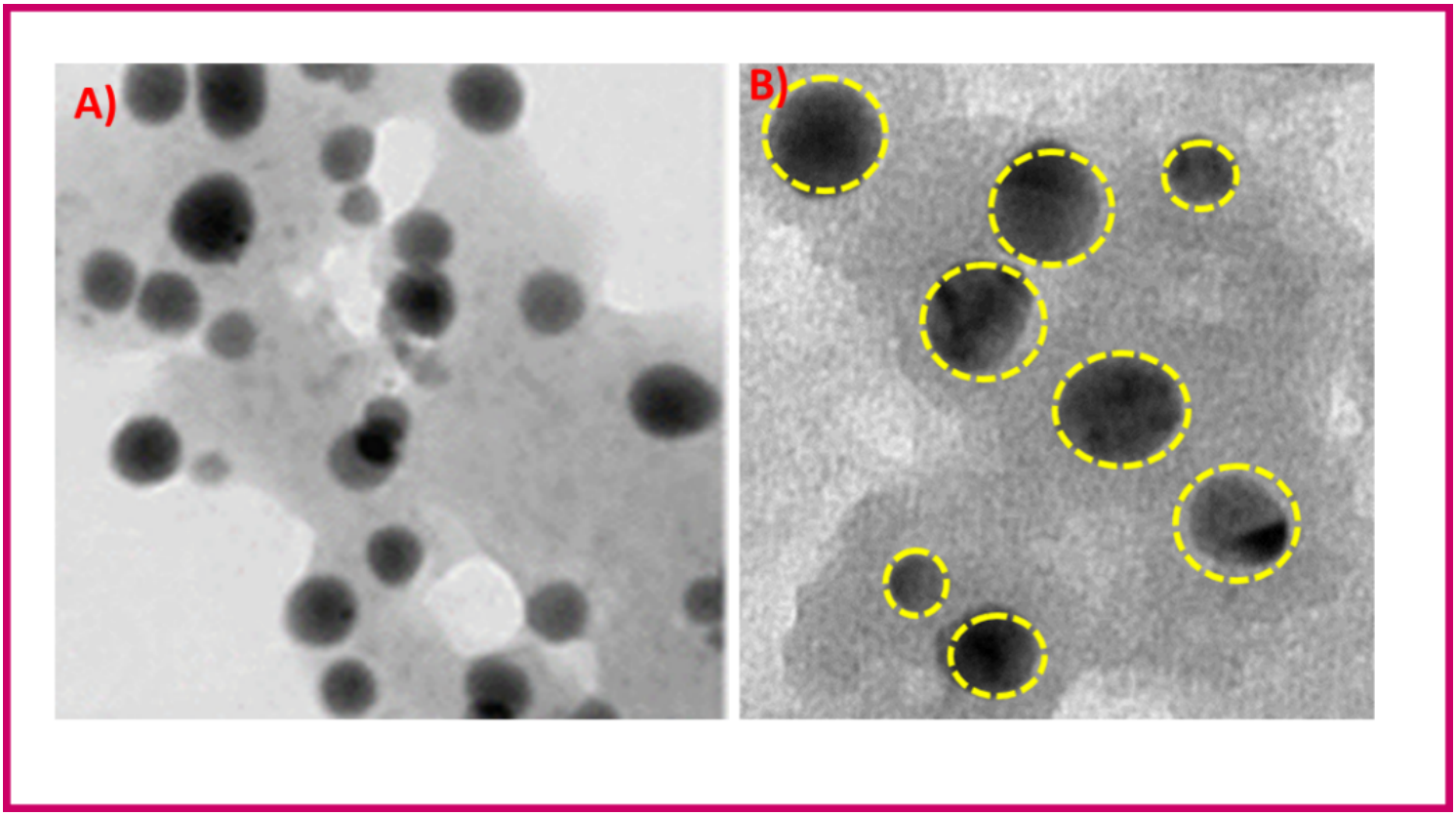

Figure 5

A) TEM image of PEG/TA-Se NPs B) Se NPs in spherical shape.

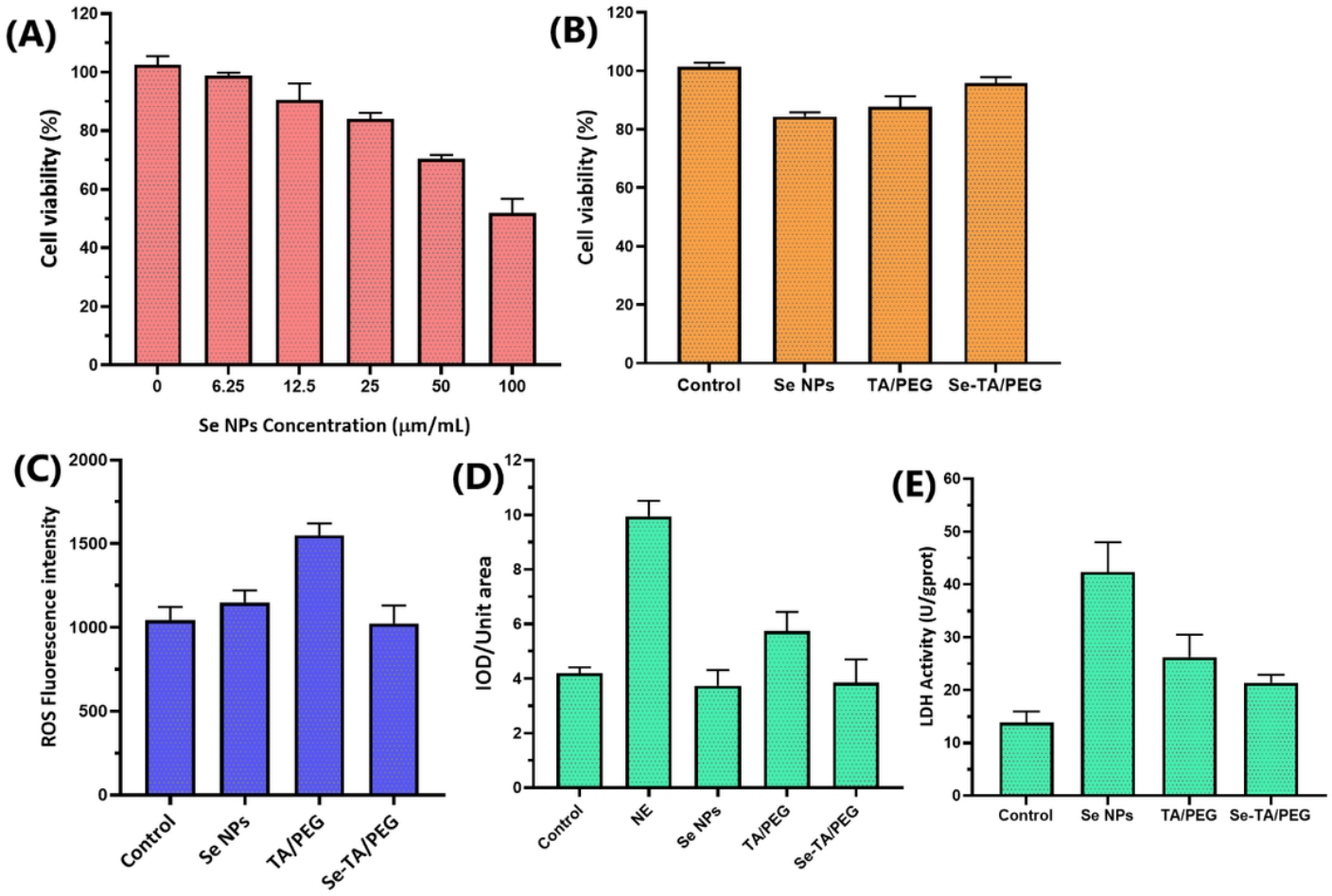

Figure 6

Investigation of cell viability on cardiomyocytes in different concentrations of Se NPs (A) and different mixture of hydrogel and control samples (B); Oxidative stress activity was examined by ROS level (C) and image optical density (D) and LDH activity measurement results (E).

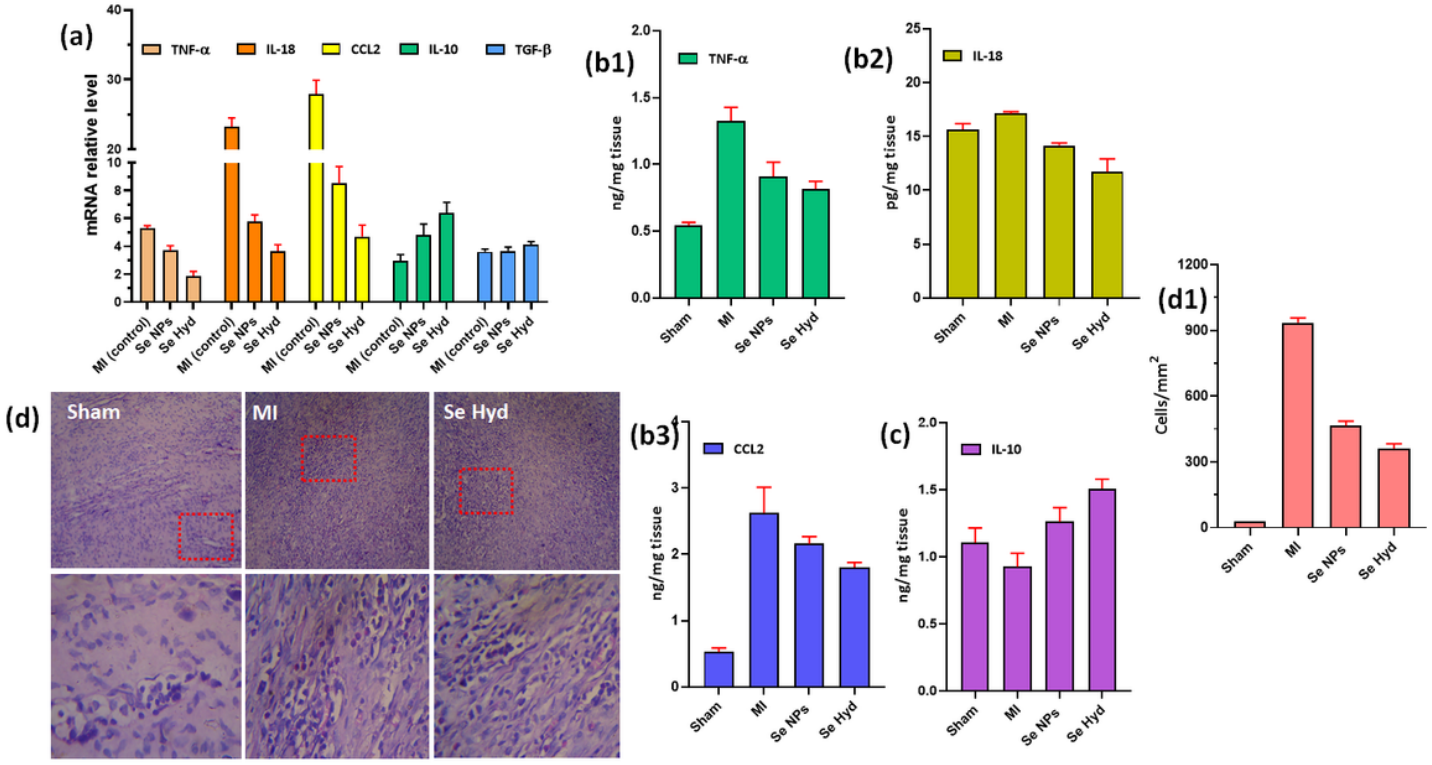

Figure 7

Effect of Se NPs loaded hydrogel samples on the inflammation factors and cytokines and macrophages infiltration examination in vivo method; (a) Quantitative measurements of mRNA level of pro-inflammatory cytokines and anti-inflammatory cytokines with treatment of control (MI), Se NPs and Se hydrogel samples. (b1, b2, b3 and c) quantitative analysis of protein levels of pro-inflammatory and anti-inflammatory cytokines investigated by ELISA method and (d & d1) visualisation on respective histological images of macrophages cells infiltration after treatment of hydrogel samples and quantification value of macrophages cells.

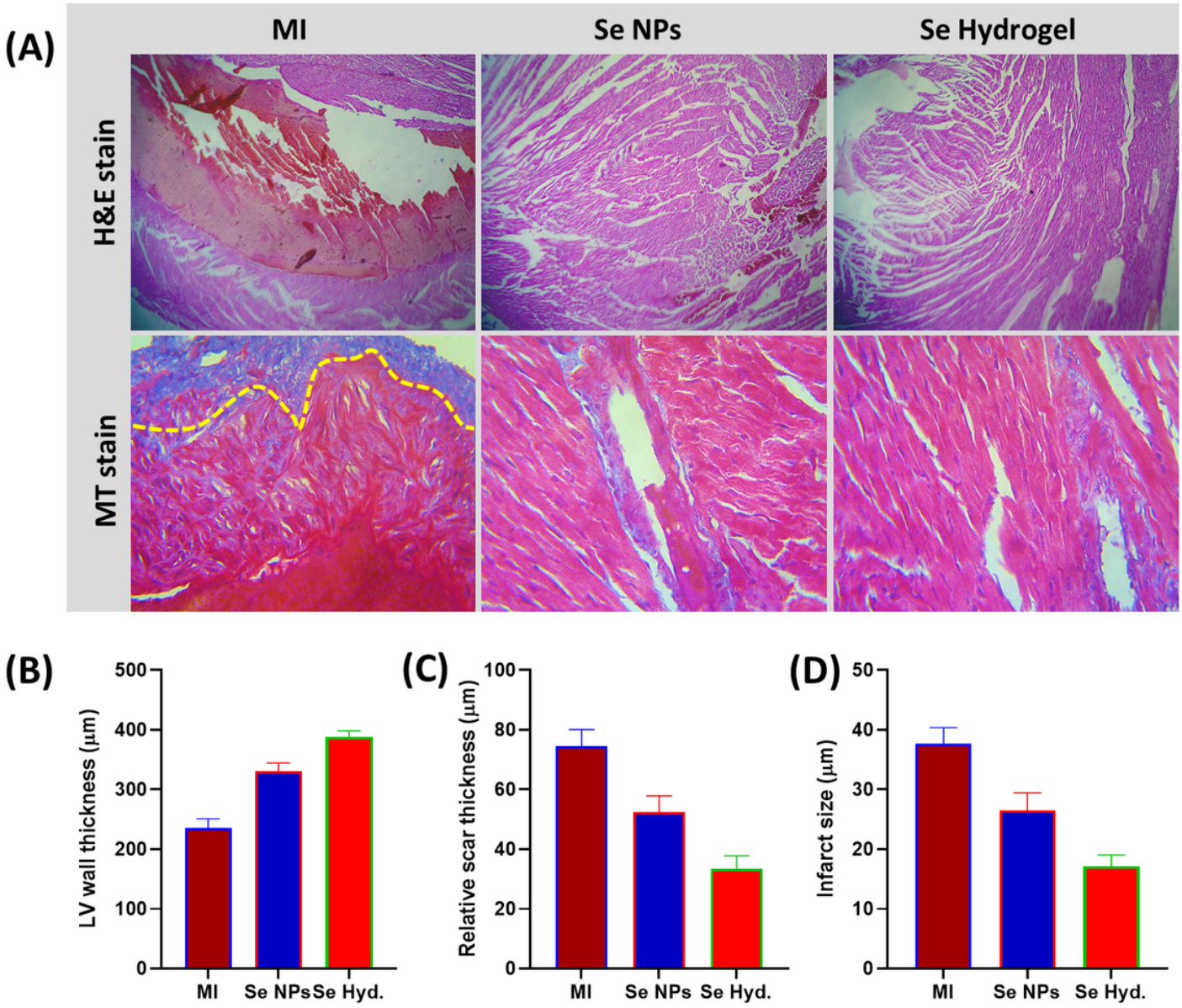

Figure 8

The investigative results of heart morphology and functional recovery after MI treated with Se NPs and Se hydrogels; (A) The respective Hematoxyline and Eosin (H&E) and Masson's Trichrome-stained MI induced cross-sections of Se NPs and Se hydrogels injected MI models (scale = 4X); (B-D) Quantitative data of ventricular wall thickness (LV), relative scar thickness and infarct size (n=3 for MI and each n=6 for Se NPs and Se hydrogels, respectively).

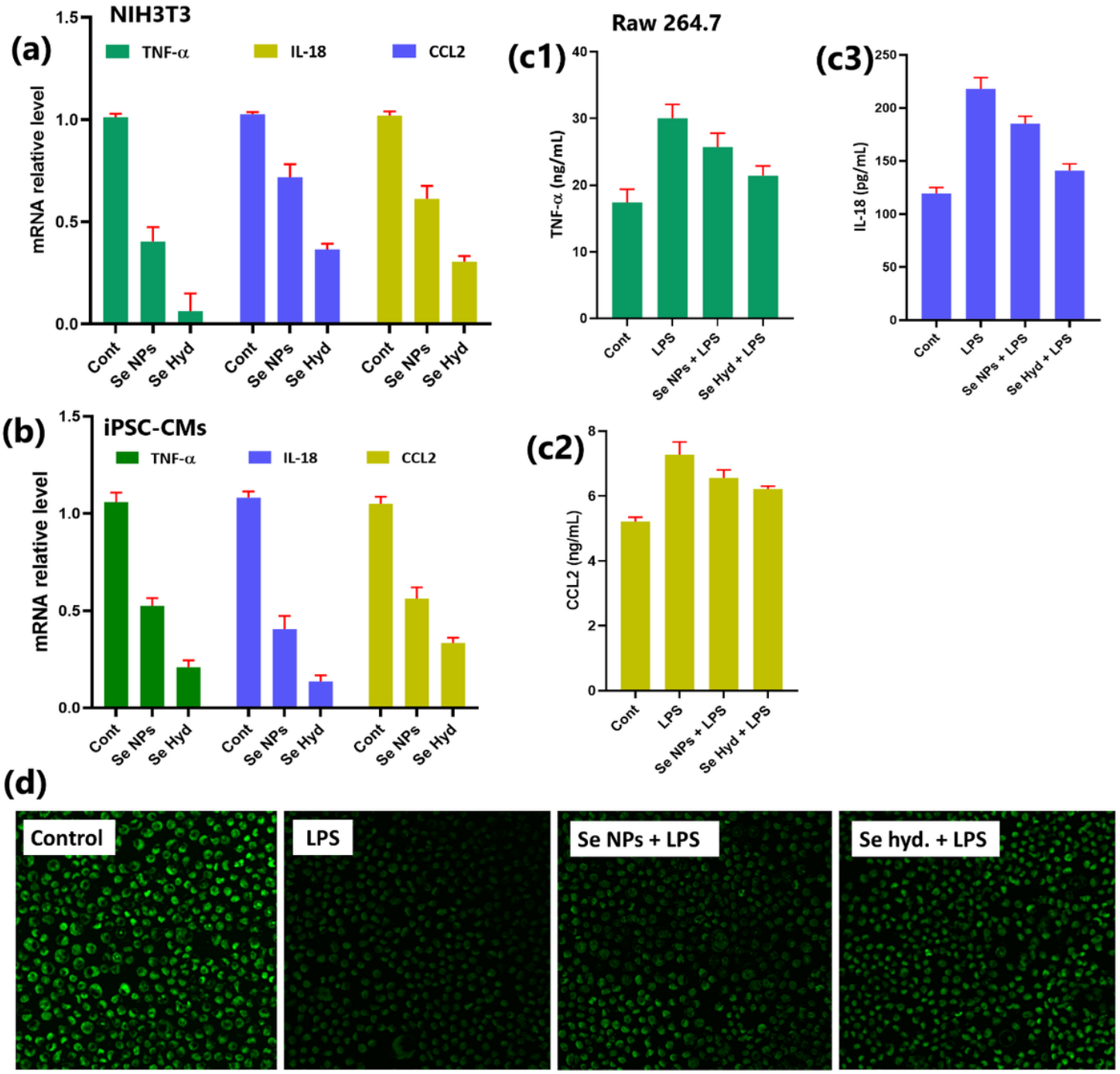

Figure 9

Examinations of Se NPs loaded hydrogel samples on the pro-inflammatory and anti-inflammatory cytokines in vitro method by using cell types of NIH3T3 (a), iPSC-CMs (b) (cardiomyocytes) and Raw 264.7 (c1, c2 & c3) macrophages; CLSM visualizations of Raw 264.7 macrophages after treatment of LPS and prepared samples to examine regenerative ability in the cardiac healing.

Supplementary Files

This is a list of supplementary files associated with this preprint. Click to download.

- Graphicalabstract.tiff